CONDENSED MATTER PHYSICS

10.1126/sciadv.1501870

Large anomalous Hall effect driven by a nonvanishing Berry curvature in the noncolinear antiferromagnet Mn_3Ge

Ajaya K. Nayak,[1,2]* Julia Erika Fischer,[1] Yan Sun,[1] Binghai Yan,[1] Julie Karel,[1] Alexander C. Komarek,[1] Chandra Shekhar,[1] Nitesh Kumar,[1] Walter Schnelle,[1] Jürgen Kübler,[3] Claudia Felser,[1] Stuart S. P. Parkin[2]*

It is well established that the anomalous Hall effect displayed by a ferromagnet scales with its magnetization. Therefore, an antiferromagnet that has no net magnetization should exhibit no anomalous Hall effect. We show that the noncolinear triangular antiferromagnet Mn_3Ge exhibits a large anomalous Hall effect comparable to that of ferromagnetic metals; the magnitude of the anomalous conductivity is ~500 $(ohm{\cdot}cm)^{-1}$ at 2 K and ~50 $(ohm{\cdot}cm)^{-1}$ at room temperature. The angular dependence of the anomalous Hall effect measurements confirms that the small residual in-plane magnetic moment has no role in the observed effect except to control the chirality of the spin triangular structure. Our theoretical calculations demonstrate that the large anomalous Hall effect in Mn_3Ge originates from a nonvanishing Berry curvature that arises from the chiral spin structure, and that also results in a large spin Hall effect of 1100 $(\hbar/e)$ $(ohm{\cdot}cm)^{-1}$, comparable to that of platinum. The present results pave the way toward the realization of room temperature antiferromagnetic spintronics and spin Hall effect–based data storage devices.

INTRODUCTION

In a normal conductor, the Lorentz force gives rise to the Hall effect, wherein the induced Hall voltage varies linearly with the applied magnetic field. Moreover, in a ferromagnetic material, one can realize a large spontaneous Hall effect—termed the anomalous Hall effect (AHE)—that scales with its magnetization (*1*, *2*). Although the detailed origin of the AHE has been puzzling for many years, recent theoretical developments have provided a deeper understanding of the intrinsic contribution of the AHE in ferromagnets in terms of the Berry-phase curvature (*1*, *3*–*6*). The Berry phase is a very useful tool for understanding the evolution of an electron's wave function in the presence of a driving perturbation, such as an electric field. The electron's motion may deviate from its usual path, wherein the electron follows a path along the direction of the applied electric field, and may pick up a transverse component of momentum even in the absence of an external magnetic field, leading to a Hall effect. This process can be understood by calculating the Berry curvature, which is an intrinsic property of the occupied electronic states in a given crystal with a certain symmetry, and only takes a nonzero value in systems where time-reversal symmetry is broken (for example, by the application of a magnetic field) or where magnetic moments are present. From symmetry analysis, the Berry curvature vanishes for conventional antiferromagnets with colinear moments, thereby resulting in zero AHE. However, a nonvanishing Berry phase in antiferromagnets with a noncolinear spin arrangement was recently predicted to lead to a large AHE (*7*–*9*). In particular, Chen *et al.* (*7*) have demonstrated theoretically that an anomalous Hall conductivity (AHC) larger than 200 $(ohm{\cdot}cm)^{-1}$ can be obtained in the noncolinear antiferromagnet Mn_3Ir.

The Heusler compound Mn_3Ge is known to crystallize in both tetragonal and hexagonal structures, depending on the annealing temperature (*10*, *11*). Hexagonal Mn_3Ge exhibits a triangular antiferromagnetic structure with an ordering temperature of ~365 to 400 K (*11*–*14*). As shown in Fig. 1A, the hexagonal unit cell of Mn_3Ge consists of two layers of Mn triangles stacked along the *c* axis. In each layer, the Mn atoms form a Kagome lattice, with Ge sitting at the center of a hexagon. Neutron diffraction studies have revealed a noncolinear triangular antiferromagnetic spin arrangement of the Mn spins in which the neighboring moments are aligned in-plane at an angle of 120° (*13*, *14*). These same studies have reported that the spin triangle is free to rotate in an external magnetic field (*13*, *14*). This noncolinear structure arises as a result of the geometrical frustration of the Mn moments that are arranged in a triangular configuration in the *a*-*b* plane. We have performed ab initio calculations of the magnetic ground state of Mn_3Ge. The lowest energy spin configuration is shown in Fig. 1B and is consistent with previous calculations (*15*, *16*). In addition to the 120° ordered antiferromagnetic structure, a very small net in-plane moment exists as a result of a small tilting of the Mn moments (*13*).

RESULTS AND DISCUSSION

We have calculated the Berry curvature and AHC in Mn_3Ge using the linear-response Kubo formulism (*1*) based on our calculated magnetic structure (Fig. 1B). We find that the AHC exhibits nearly zero values for both *xy* (σ^z_{xy}) and *yz* (σ^x_{yz}) components and only large values for the *xz* component σ^y_{xz} = 330 $(ohm{\cdot}cm)^{-1}$. Here, σ^k_{ij} corresponds to the AHC when current flows along the *j* direction, and thereby results in a Hall voltage along the *i* direction: σ^k_{ij} can be treated as a pseudovector pointing along the *k* direction that is perpendicular to both the *i* direction and the *j* direction. The symmetry of the antiferromagnetic structure of Mn_3Ge determines which components of the AHC tensor must be zero. As shown in Fig. 1, the two magnetic layers that compose the primitive unit cell of the antiferromagnetic structure of Mn_3Ge can be transformed into each other by a mirror reflection, with respect to the *xz* plane (as indicated in Fig. 1), plus a translation by *c*/2 along the *c* axis. Because of the mirror symmetry, the components

[1]Max Planck Institute for Chemical Physics of Solids, Nöthnitzer Str. 40, 01187 Dresden, Germany. [2]Max Planck Institute of Microstructure Physics, Weinberg 2, D-06120 Halle, Germany. [3]Institut für Festkörperphysik, Technische Universität Darmstadt, 64289 Darmstadt, Germany.
*Corresponding author. E-mail: nayak@cpfs.mpg.de (A.K.N.); stuart.parkin@mpi-halle.mpg.de (S.S.P.P.)

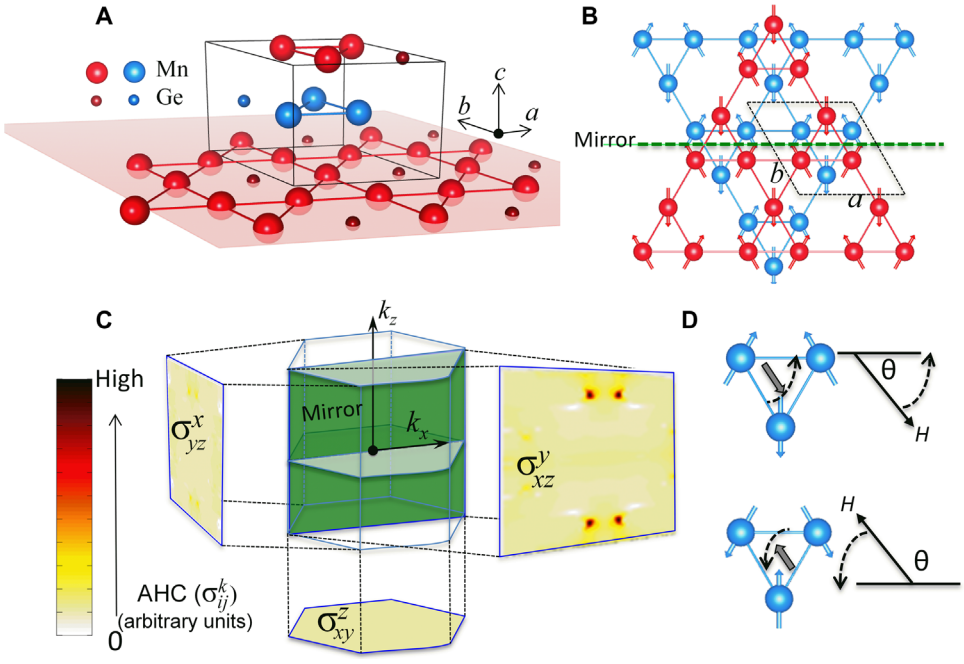

Fig. 1. Crystal structure, magnetic structure, and Berry curvature of Mn_3Ge. (**A**) Crystal structure showing the two layers of Mn-Ge atoms stacked along the *c*(*z*) axis. Red and blue spheres represent atoms lying in the $z = 0$ and $z = c/2$ planes, respectively. Large and small spheres represent Mn and Ge atoms, respectively. In each layer, the Mn atoms form a Kagome-type lattice. (**B**) Calculated 120° antiferromagnetic configuration in the $z = 0$ and $z = c/2$ planes, respectively. Only the Mn atoms are shown, with their moments represented by arrows. The green dashed line indicates the mirror plane (that is, the *xz* plane). Corresponding mirror reflection plus a translation by *c*/2 along the *z* axis transforms the system back into itself, by exchanging two magnetic planes. (**C**) First Brillouin zone and momentum-dependent AHC. The mirror plane (that is, $k_x - k_z$ plane) is highlighted in green. The component of the AHC tensor (σ_{ij}^{k}) is shown in the $k_i - k_j$ plane, which corresponds to the Berry curvature of all occupied electronic states integrated over the k_k direction. Here, only the σ_{xz}^{y} component exhibits large values. (**D**) Illustration of the rotation of the triangular spin structure with an in-plane field. There is a small in-plane net magnetic moment that we calculate to be along the direction indicated. When the field (*H*) rotates by 180°, the chiral spin structure can be reversed, resulting in the sign change in the AHC.

of the σ_{ij}^{k} vanish if they align parallel to the mirror plane. This is the case for σ_{xy}^{z} and σ_{yz}^{x}, which are expected to be exactly zero. However, the aforementioned residual net in-plane moment acts as a perturbation of the mirror symmetry. As a consequence, σ_{xy}^{z} and σ_{yz}^{x} can pick up nonzero but tiny values. By contrast, the component of σ_{ij}^{k} perpendicular to the mirror plane (namely, σ_{xz}^{y}) is nonzero. We show the calculated values of σ_{xz}^{y} in the *xz* plane in Fig. 1D. The distribution is highly nonuniform and is characterized by four well-defined peaks (that is, "hot spots"). These peaks correspond to regions in *k* space where there is a small energy gap between the occupied bands and the empty bands: this small gap is a consequence of the spin-orbit coupling within the Mn 3d band.

Moreover, a large AHC [~900 $(\text{ohm}\cdot\text{cm})^{-1}$] has previously been shown theoretically by considering a slightly different spin configuration (*8*). In the latter case, a nonvanishing component of the AHC can be obtained in the *yz* plane. The reason for this difference is straightforward; in the spin configuration shown in Fig. 1B, if the spins parallel to *y* tilt slightly in the *x* direction, a nonzero Berry curvature in the *yz* plane will result. In all of these configurations, the AHE is zero in the *xy* plane if one strictly considers only an in-plane spin structure. We note that other noncolinear spin structures, including a 120° spin structure on a triangular lattice, can also give rise to an AHE (*9*).

Like the AHE, the intrinsic spin Hall effect also originates from the band structure. The strong entanglement between occupied and unoccupied states near the Fermi level should give rise to a large contribution to both anomalous and spin Hall conductivities. Motivated by our large AHC, we have also theoretically analyzed the spin Hall conductivity (SHC), and we predict that a large SHC of 1100 (ħ/e) $(\text{ohm}\cdot\text{cm})^{-1}$ can be obtained in Mn_3Ge. The theoretical SHC in Mn_3Ge is comparable to that of Pt (*17*) and is larger than the SHC recently reported in Mn_3Ir, which also exhibits a triangular antiferromagnetic structure (*18*). In the present work, we experimentally show evidence for an AHC in a hexagonal single crystal of Mn_3Ge that agrees well with our theoretical predictions of AHC.

To probe the AHE in Mn_3Ge, we have carried out detailed Hall effect measurements as a function of magnetic field over temperatures varying from 2 to 400 K. Figure 2A shows the Hall resistivity ρ_H versus the magnetic field *H* measured for the current (*I*) along [0001] and (*H*) parallel to [01-10]. ρ_H saturates in modest magnetic fields, attaining a large saturation value of 5.1 μohm·cm at 2 K and ~1.8 μohm·cm at 300 K. The Hall conductivity for the same *I* and *H* configurations (which we label configuration I) (σ_{xz}), calculated from $\sigma_H = -\rho_H/\rho^2$ (where ρ is the normal resistivity), exhibits a large value of ~500 $(\text{ohm}\cdot\text{cm})^{-1}$ at 2 K and a modest value of ~50 $(\text{ohm}\cdot\text{cm})^{-1}$ at 300 K (Fig. 2B). Because both ρ_H and σ_H saturate in magnetic fields, these clearly reflect an AHE that is large in magnitude. To study whether the experimental AHE has an anisotropy, as predicted by theory, we measured ρ_H with *I* along [01-10] and with *H* parallel to [2-1-10] (σ_{yz}). In this

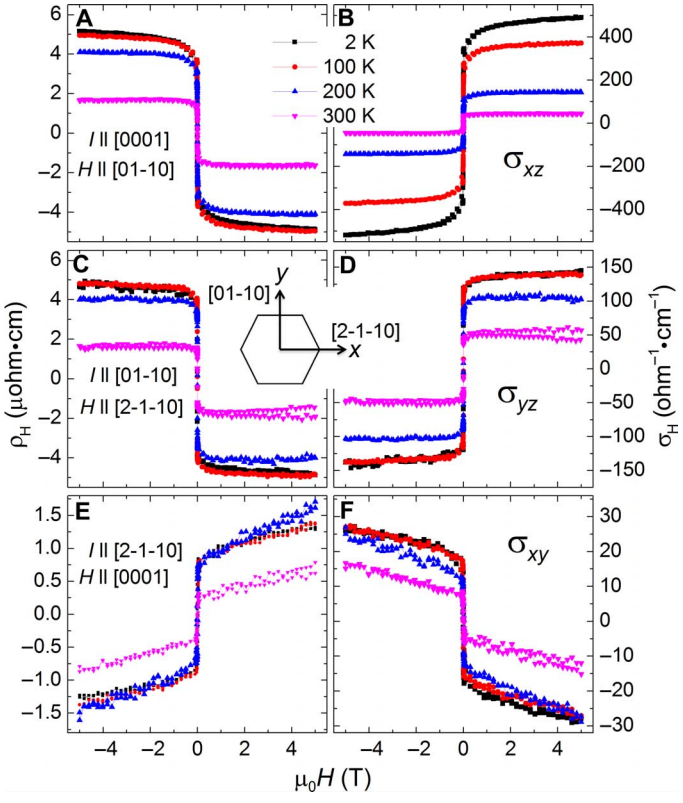

Fig. 2. AHE. (**A** to **F**) Hall resistivity (ρ_H) (A, C, and E) and Hall conductivity (σ_H) (B, D, and F) as a function of magnetic field (*H*), measured at four representative temperatures between 2 and 300 K, for three different current and magnetic field configurations. The hexagon in the inset to (C) and (D) shows the two in-plane directions used for the current and magnetic field in the present measurements.

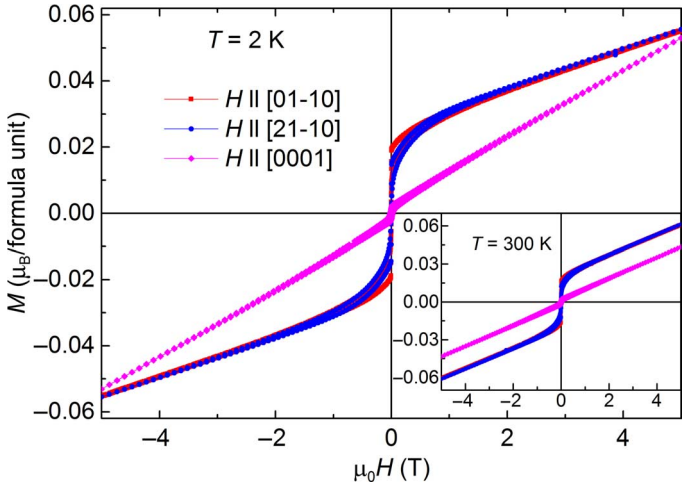

Fig. 3. Magnetic properties. Field dependence of magnetization *M* (*H*) measured at 2 K, with the field parallel to the three orientations used in the AHE measurements. The inset shows *M* (*H*) loops measured at 300 K.

configuration II, ρ_H is slightly smaller than configuration I (~4.8 μohm·cm at 2 K and 1.6 μohm·cm at 300 K) (Fig. 2C). Although σ_H (σ_{yz}) is reduced at 2 K in configuration II compared to configuration I [to about 150 $(ohm·cm)^{-1}$], a similar value of σ_H = 50 $(ohm·cm)^{-1}$ at 300 K is found for both configuration I and configuration II (Fig. 2D). In both cases, ρ_H is negative (positive) for positive (negative) fields. Finally, in a third configuration (configuration III), we apply *I* along [2-1-10] and *H* parallel to [0001]. In this configuration, we observe small values of both ρ_H and σ_H (σ_{xy}) at all temperatures (Fig. 2, E and F); moreover, the sign of AHE is opposite to that for configurations I and II.

To confirm that the observation of a large AHE in the present system originates from the noncolinear antiferromagnetic spin structure, we have performed magnetization measurements with the field parallel to different crystallographic directions. The temperature dependence of magnetization *M* (*T*) indicates a T_C of 380 K for the present Mn_3Ge single crystal (see the Supplementary Materials), only slightly lower than that reported in the literature. The *M* (*H*) loop measured with the field parallel to [2-1-10] displays a tiny spontaneous magnetization of 0.005 μ_B/Mn at 2 K (Fig. 3). The zero field moment is slightly larger (0.006 μ_B/Mn at 2 K) when the field is applied parallel to [01-10]. An extremely soft magnetic behavior is found in both cases, with coercive fields (H_C) of less than 20 Oe. These magnetization values agree well with previous results that show an in-plane magnetic moment of ~0.007 μ_B/Mn (*12*). Although the Mn moments are expected to lie only in the *a*-*b* plane, we observe a moment that is an order of magnitude less than 0.0007 μ_B/Mn at 2 K for a field parallel to [0001]. This indicates that there could be a very small tilting of the Mn spins toward the *c* axis. The *M* (*H*) loops measured at 300 K for different field orientations are similar to the 2 K data, except that the high-field magnetization strongly decreases for *H* parallel to [0001] (inset to Fig. 3).

From our magnetization data, it is clear that the present Mn_3Ge sample has a nearly zero net magnetic moment. Hence, we conclude that the extremely large AHE depicted in Fig. 2 must be related to the noncolinear antiferromagnetic spin structure, as predicted by theory. The observation of a large AHC in the *xz* and *yz* planes, and of a very small effect in the *xy* plane, is also consistent with our theoretical calculations. Although our calculations show a nonzero AHC only in the *xz* plane, this is true for the particular spin configuration considered (see Fig. 1B). By symmetry, the *x* and *y* directions must be symmetry-related so that there will be equal contributions to the measured AHE for the various symmetry-related spin configurations (by rotation by ±120° in Fig. 1B) or the spin configurations can be rotated by the applied field as a result of the small in-plane magnetic moment, as illustrated in Fig. 1D.

It is interesting to compare the magnitude of the present AHE with that exhibited by ferromagnetic Heusler compounds because the hexagonal Mn_3Ge structure evolves from the cubic Heusler structure by distortion of the lattice along the (111) direction. For example, the ferromagnetic Heusler compounds Co_2MnSi and Co_2MnGe, which exhibit a net magnetic moment of ~5 μ_B/Mn (more than two orders of magnitude higher by comparison to the present h-Mn_3Ge), display a maximum ρ_H of ~4 μohm·cm (*19*). The same study showed that ρ_H decreases by two orders of magnitude when the magnetization is reduced to nearly half in Cu_2MnAl (*19*). A similar scaling of ρ_H with magnetization has also been demonstrated by Zeng *et al.* (*2*) for ferromagnetic Mn_5Ge_3. Moreover, it has also been well established that the Hall conductivity in many ferromagnetic materials scales with their normal conductivity (*19*–*21*). In the present case, the Hall conductivity measured with the current along different crystallographic directions

follows a behavior similar to that of the normal conductivity (see the Supplementary Materials). Similar data for the AHE in the noncolinear antiferromagnet Mn_3Sn have been recently published by Nakatsuji *et al.* (*22*). However, Mn_3Ge exhibits distinctions in its magnetism, as well as its AHE, in comparison to Mn_3Sn. In particular, the maximum AHC in the present system is nearly three times higher than that of Mn_3Sn. Moreover, Mn_3Ge does not show any secondary transition, such as the cluster glass phase observed at low temperatures in Mn_3Sn (*22*).

According to theoretical predictions, the nonvanishing Berry curvature arising from the noncolinear triangular antiferromagnetic structure is responsible for the observed large AHE. In such a scenario, we would expect to observe an AHE without applying any magnetic field. However, the special spin arrangement in both h-Mn_3Ge and h-Mn_3Sn can lead to the formation of antiferromagnetic domains. Therefore, in zero magnetic field, the direction of the Hall voltage may be different in each antiferromagnetic domain, resulting in a vanishing AHC. The presence of a weak in-plane ferromagnetic moment ensures that a small magnetic field in one direction within the *a*-*b* plane is sufficient to eliminate the domains, and hence allows the establishment of a large AHE. In particular, neutron diffraction measurements have established that an applied magnetic field does not substantially affect the 120° triangular antiferromagnetic spin structure, but the magnetic field does result in a rotation of the spin triangle opposite to the in-plane field component (*14*, *23*). Therefore, switching the direction of an in-plane field from positive to negative results in the switching of the direction of the staggered moment in the triangular spin structure, and consequently causes a change in the sign of the anomalous Hall voltage. The small variation of the anomalous Hall signal at high fields likely originates from the normal component of the Hall signal or from the magnetic susceptibility of the magnetic structure.

To establish that the presence of the weak in-plane ferromagnetism in Mn_3Ge has virtually no role in the observed AHE, we have carried out angular-dependent measurements of the AHE for various field and current configurations. In configuration I shown in Fig. 4A, the current was applied along *z* and the voltage was measured in the *xz* plane, resulting in V_x. In this configuration, the initial field direction for $\theta = 0$ is along *y*. The field was then rotated in the *y*-*z* plane. Under these conditions, the AHC (σ_{yz}) remains constant up to $\theta = 90°$, where it suddenly changes sign. A similar sign change occurs again at $\theta = 270°$. This behavior can be explained as follows: with increasing θ, although the in-plane magnetic field decreases, a small component of the field lies parallel to the *a*-*b* plane up to $\theta = 90°$. This small in-plane field maintains the chirality of the triangular spin structure in a single direction. At angles greater than 90°, the in-plane field changes its direction, resulting in a change in the chirality of the spin structure, which produces the sign change in the AHE. A similar phenomenon happens at 270° (Fig. 4B). In configuration II, we apply the current along *y* with the voltage measured in the *yz* plane (V_z), and the field is rotated in the *x*-*z* plane. In this case, *H* is always perpendicular to *I*. The angular dependence of the AHC (σ_{yz}) follows the same behavior as that of configuration I. In both cases, a large and constant AHC was obtained when at least a small field parallel to the in-plane spin structure was present. We now show that the AHC measured in the *xy* plane (σ_{xy}) always remains nearly zero even when there is a nonzero field component parallel to the plane of the triangular spin structure. In configuration III, V_y was measured in the *xy* plane with *I* along *x* (Fig. 4C). The field was rotated in the *z*-*y* plane. In this configuration, a component of the magnetic field always remains parallel to the *a*-*b* plane, except for $\theta = 0$ and 180°. However, σ_{xy} remains nearly zero regardless of the field direction. A small nonvanishing value of σ_{xy} may appear from a slight canting of the spins along the *z* (*c*) direction. The feasibility of a nonplanar structure in Mn_3Ge has also been discussed in our previous theoretical work (*8*). From these angle-dependent measurements, it can be readily concluded that the small residual in-plane ferromagnetic component, as well as the applied magnetic field, plays no role in the observed large AHE in Mn_3Ge.

In summary, we have experimentally demonstrated that the noncolinear antiferromagnet Mn_3Ge exhibits a large AHE, even at room temperature. The origin of this exotic effect is discussed in terms of a nonvanishing Berry curvature in momentum space. Antiferromagnets are of significant interest for spintronic applications (*24*–*26*) because, in contrast to ferromagnets, they do not produce any undesirable dipole fields. Therefore, the present antiferromagnetic material with a large AHE, which is easily controlled by the current, can be exploited for spintronics, without the drawbacks of ferromagnets. Finally, our theoretical finding of a large spin Hall effect in Mn_3Ge will motivate

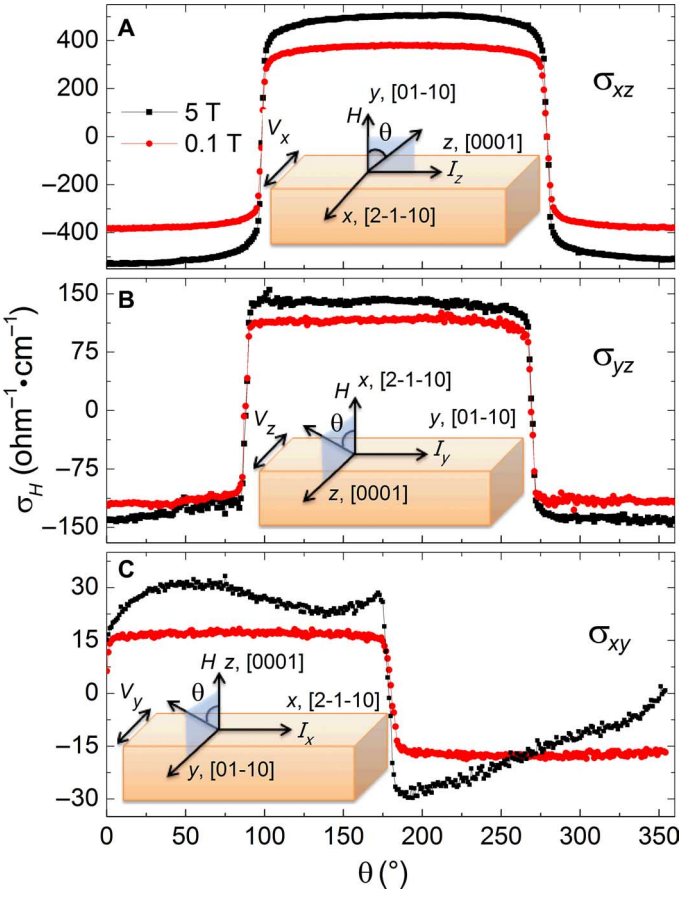

Fig. 4. Angular dependence of AHE. Angular (θ) dependence of the AHC measured for the three current and field configurations used in Fig. 2. A schematic diagram of the sample geometry is shown for each configuration. (**A** to **C**) The rotation was performed along (A) *y*-*z* for *I* along *z* [0001], (B) *x*-*z* for *I* along *y* [01-10], and (C) *y*-*z* for *I* along *x* [2-1-10]. $\theta = 0$ corresponds to *H* oriented along *y*, *x*, and *z* in (A), (B), and (C), respectively. We have used the same *x*, *y*, *z* coordinates as shown in the theoretical spin arrangement in Fig. 1B.

further studies to explore other phenomena derived from the Berry-phase curvature in antiferromagnets.

During the writing of the present manuscript, we became aware of a similar study of a large AHE in Mn_3Sn conducted by Nakatsuji *et al.* (*22*). We have compared the present findings for Mn_3Ge with those for Mn_3Sn in the main text.

MATERIALS AND METHODS

For the single-crystal growth, stoichiometric quantities of pure elements were weighed and premelted in an alumina crucible in an induction furnace. The ingot was ground and put in an alumina crucible, which was sealed in a quartz ampule. The single crystal was grown using the Bridgman-Stockbarger technique. The growth temperature was controlled at the bottom of the ampule. The material was heated up to 980°C, remained there for 1 hour to ensure homogeneity of the melt, and was cooled down slowly to 740°C. The sample was annealed at 740°C for 15 hours and then quenched to room temperature in argon gas. The sample was cut into five slices perpendicular to the growth direction. The dimensions of each slice were approximately 6 mm in diameter and 2 mm thick. Single-crystal x-ray diffraction was carried out on a Bruker D8 VENTURE x-ray diffractometer using Mo-K radiation and a bent graphite monochromator. The magnetization measurements were carried out on a vibrating sample magnetometer (MPMS 3, Quantum Design). The transport measurements were performed with low-frequency alternating current (ACT option, PPMS 9, Quantum Design). Our ab initio density functional theory calculations were performed using the Vienna Ab-initio Simulation Package with projected augmented wave potential (*27*). The exchange-correlation energy was considered at the generalized gradient approximation level (*28*). Further details of the calculations are given in the Supplementary Materials.

SUPPLEMENTARY MATERIALS

Supplementary material for this article is available at http://advances.sciencemag.org/cgi/content/full/2/4/e1501870/DC1

fig. S1. Temperature dependence of magnetization.

fig. S2. Conductivity with temperature.

REFERENCES AND NOTES

1. N. Nagaosa, J. Sinova, S. Onoda, A. H. MacDonald, N. P. Ong, Anomalous Hall effect. *Rev. Mod. Phys.* **82**, 1539–1592 (2010).
2. C. Zeng, Y. Yao, Q. Niu, H. H. Weitering, Linear magnetization dependence of the intrinsic anomalous Hall effect. *Phys. Rev. Lett.* **96**, 037204 (2006).
3. Y. Taguchi, Y. Oohara, H. Yoshizawa, N. Nagaosa, Y. Tokura, Spin chirality, Berry phase, and anomalous Hall effect in a frustrated ferromagnet. *Science* **291**, 2573–2576 (2001).
4. Z. Fang, N. Nagaosa, K. S. Takahashi, A. Asamitsu, R. Mathieu, T. Ogasawara, H. Yamada, M. Kawasaki, Y. Tokura, K. Terakura, The anomalous Hall effect and magnetic monopoles in momentum space. *Science* **302**, 92–95 (2003).
5. T. Jungwirth, Q. Niu, A. H. MacDonald, Anomalous Hall effect in ferromagnetic semiconductors. *Phys. Rev. Lett.* **88**, 207208 (2002).
6. Y. Yao, L. Kleinman, A. H. MacDonald, J. Sinova, T. Jungwirth, D.-S. Wang, E. Wang, Q. Niu, First principles calculation of anomalous Hall conductivity in ferromagnetic bcc Fe. *Phys. Rev. Lett.* **92**, 037204 (2004).
7. H. Chen, Q. Niu, A. H. MacDonald, Anomalous Hall effect arising from noncollinear antiferromagnetism. *Phys. Rev. Lett.* **112**, 017205 (2014).
8. J. Kübler, C. Felser, Non-collinear antiferromagnets and the anomalous Hall effect. *Europhys. Lett.* **108**, 67001 (2014).
9. R. Shindou, N. Nagaosa, Orbital ferromagnetism and anomalous Hall effect in antiferromagnets on the distorted fcc lattice. *Phys. Rev. Lett.* **87**, 116801 (2001).
10. T. Ohoyama, X-ray and magnetic studies of the manganese-germanium system. *J. Phys. Soc. Jpn.* **16**, 1995–2002 (1961).
11. J. F. Qian, A. K. Nayak, G. Kreiner, W. Schnelle, C. Felser, Exchange bias up to room temperature in antiferromagnetic hexagonal Mn_3Ge. *J. Phys. D Appl. Phys.* **47**, 305001 (2014).
12. N. Yamada, H. Sakai, H. Mori, T. Ohoyama, Magnetic properties of ϵ-Mn_3Ge. *Physica B+C* **149**, 311–315 (1988).
13. S. Tomiyoshi, Y. Yamaguchi, T. Nagamiya, Triangular spin configuration and weak ferromagnetism of Mn_3Ge. *J. Magn. Magn. Mater.* **31–34**, 629–630 (1983).
14. T. Nagamiya, S. Tomiyoshi, Y. Yamaguchi, Triangular spin configuration and weak ferromagnetism of Mn_3Sn and Mn_3Ge. *Solid State Commun.* **42**, 385–388 (1982).
15. D. Zhang, B. Yan, S.-C. Wu, J. Kübler, G. Kreiner, S. S. P. Parkin, C. Felser, First-principles study of the structural stability of cubic, tetragonal and hexagonal phases in Mn_3Z (Z=Ga, Sn and Ge) Heusler compounds. *J. Phys. Condens. Matter* **25**, 206006 (2013).
16. L. M. Sandratskii, J. Kübler, Role of orbital polarization in weak ferromagnetism. *Phys. Rev. Lett.* **76**, 4963–4966 (1996).
17. G. Y. Guo, S. Murakami, T.-W. Chen, N. Nagaosa, Intrinsic spin Hall effect in platinum: First-principles calculations. *Phys. Rev. Lett.* **100**, 096401 (2008).
18. W. Zhang, W. Han, S.-h. Yang, Y. Sun, Y. Zhang, B. Yan, S. S. P. Parkin, Facet-dependent giant spin orbit torque in single crystalline antiferromagnetic Ir-Mn/ferromagnetic permalloy bilayers. arXiv:1602.00670 (2015).
19. M. Obaida, K. Westerholt, H. Zabel, Magnetotransport properties of Cu_2MnAl, Co_2MnGe, and Co_2MnSi Heusler alloy thin films: From nanocrystalline disordered state to long-range-ordered crystalline state. *Phys. Rev. B* **84**, 184416 (2011).
20. N. Manyala, Y. Sidis, J. F. DiTusa, G. Aeppli, D. P. Young, Z. Fisk, Large anomalous Hall effect in a silicon-based magnetic semiconductor. *Nat. Mater.* **3**, 255–262 (2004).
21. T. Miyasato, N. Abe, T. Fujii, A. Asamitsu, S. Onoda, Y. Onose, N. Nagaosa, Y. Tokura, Crossover behavior of the anomalous Hall effect and anomalous Nernst effect in itinerant ferromagnets. *Phys. Rev. Lett.* **99**, 086602 (2007).
22. S. Nakatsuji, N. Kiyohara, T. Higo, Large anomalous Hall effect in a non-collinear antiferromagnet at room temperature. *Nature* **527**, 212–215 (2015).
23. S. Tomiyoshi, Y. Yamaguchi, Magnetic structure and weak ferromagnetism of Mn_3Sn studied by polarized neutron diffraction. *J. Phys. Soc. Jpn.* **51**, 2478–2486 (1982).
24. A. K. Nayak, M. Nicklas, S. Chadov, P. Khuntia, C. Shekhar, A. Kalache, M. Baenitz, Y. Skourski, V. K. Guduru, A. Puri, U. Zeitler, J. M. D. Coey, C. Felser, Design of compensated ferrimagnetic Heusler alloys for giant tunable exchange bias. *Nat. Mater.* **14**, 679–684 (2015).
25. B. G. Park, J. Wunderlich, X. Martí, V. Holý, Y. Kurosaki, M. Yamada, H. Yamamoto, A. Nishide, J. Hayakawa, H. Takahashi, A. B. Shick, T. Jungwirth, A spin-valve-like magnetoresistance of an antiferromagnet-based tunnel junction. *Nat. Mater.* **10**, 347–351 (2011).
26. X. Marti, I. Fina, C. Frontera, J. Liu, P. Wadley, Q. He, R. J. Paull, J. D. Clarkson, J. Kudrnovský, I. Turek, J. Kuneš, D. Yi, J.-H. Chu, C. T. Nelson, L. You, E. Arenholz, S. Salahuddin, J. Fontcuberta, T. Jungwirth, R. Ramesh, Room-temperature antiferromagnetic memory resistor. *Nat. Mater.* **13**, 367–374 (2014).
27. G. Kresse, J. Furthmüller, Efficient iterative schemes for *ab initio* total-energy calculations using a plane-wave basis set. *Phys. Rev. B Condens. Matter* **54**, 11169–11186 (1996).
28. J. P. Perdew, K. Burke, M. Ernzerhof, Generalized gradient approximation made simple. *Phys. Rev. Lett.* **77**, 3865–3868 (1996).

Acknowledgments: We thank C. Geibel for helpful discussions and use of the Bridgman furnace. **Funding:** This work was financially supported by the Deutsche Forschungsgemeinschaft (project numbers TP 1.2-A and 2.3-A of Research Unit FOR 1464 ASPIMATT) and by the European Research Council Advanced Grant (grant 291472) "Idea Heusler." **Author contributions:** A.K.N. performed the transport and magnetic measurements with the help of C.S., N.K., and W.S. The theoretical calculations were carried out by Y.S., B.Y., and J. Kübler. J.E.F. synthesized the single crystal. J.E.F., A.C.K., and J. Karel performed the structural characterization. A.K.N. and S.S.P.P. wrote the manuscript, with substantial contributions from all authors. C.F. and S.S.P.P. inspired and jointly supervised the project. **Competing interests:** The authors declare that they have no competing interests. **Data and materials availability:** All data used to obtain the conclusions in this paper are presented in the paper and/or the Supplementary Materials. Other data may be requested from the authors. Please direct all inquiries to A.K.N. (nayak@cpfs.mpg.de) and S.S.P.P. (stuart.parkin@mpi-halle.mpg.de).

Submitted 20 December 2015
Accepted 17 March 2016
Published 15 April 2016
10.1126/sciadv.1501870

Citation: A. K. Nayak, J. E. Fischer, Y. Sun, B. Yan, J. Karel, A. C. Komarek, C. Shekhar, N. Kumar, W. Schnelle, J. Kübler, C. Felser, S. S. P. Parkin, Large anomalous Hall effect driven by a nonvanishing Berry curvature in the noncolinear antiferromagnet Mn_3Ge. *Sci. Adv.* **2**, e1501870 (2016).